Poster ID: P6-04-08

Machine learning-based characterization of the breast cancer tumor microenvironment for assessment of neoadjuvant-treatment response

STUDY BACKGROUND

Neoadjuvant treatment of breast cancer has been shown to potentially reduce the extent and morbidity of subsequent surgery. Response to neoadjuvant therapy may also be prognostic; complete pathologic response (pCR) following neoadjuvant treatment is associated with improved long-term outcomes[1]. pCR, defined as the absence of residual invasive cancer, is determined by evaluation of H&E-stained breast resections and regional lymph nodes following neoadjuvant treatment; however, pathologist assessment is subject to intra- and inter-reader variability.

Here we report machine learning (ML)-based models to identify tissue regions and cell types in the tumor microenvironment (TME) of H&E-stained breast cancer specimens. Model predictions were used to derive tumor bed area and a residual cancer burden score (RCB)-like score to assess residual disease after neoadjuvant therapy[2,3].

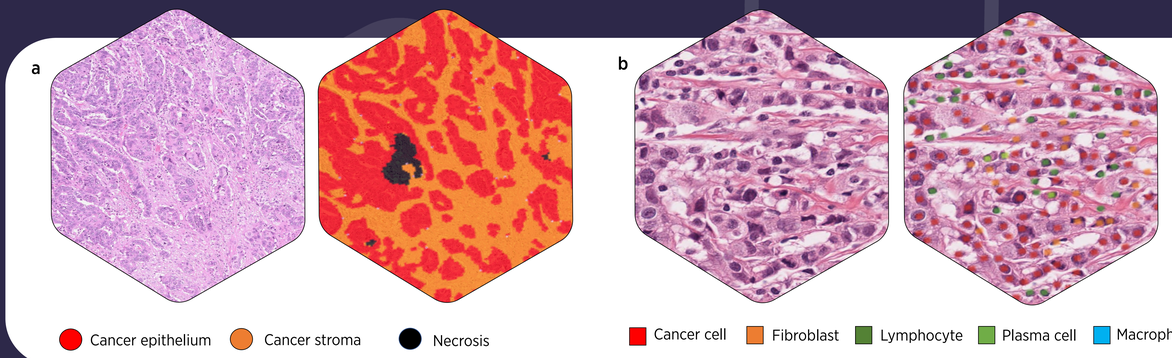

Figure 2. Example images of overlays generated by PathAI tissue and cell models deployed in breast cancer. a) H&E-stained WSI and corresponding tissue overlay. b) H&E-stained WSI and corresponding cell overlay.

METHODS

- Convolutional neural network (CNN) models were trained using 229,901 pathologist annotations on digitized H&E-stained whole slide images (WSIs) of 2700 neoadjuvant-treated breast cancer specimens (resections and biopsies) from 4 sources, and an additional 1100 breast cancer primary resections from TCGA.
- CNN models were trained to segment tissue regions (cancer epithelium, stroma, diffuse inflammatory infiltrate, ductal carcinoma in situ (DCIS), lymph nodes and necrosis) and identify cell types (cancer epithelial cells, fibroblasts, lymphocytes, macrophages, foamy macrophages and plasma cells) at single-pixel resolution (Figures 1,2).

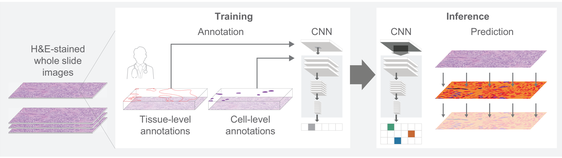

Figure 1. Schematic illustrating convolutional neural network (CNN) model development approach for pixel-level feature predictions.

- These tissue region segmentations were used to derive tumor bed area using a convex hull algorithm. Cancer cellularity was calculated as the proportion of the area of predicted DCIS in tissue + area of predicted cancer in tissue, over the total area of tissue. Tumor bed area predictions, together with cancer cellularity predictions, were then used to compute an RCB-like score (Figure 3).

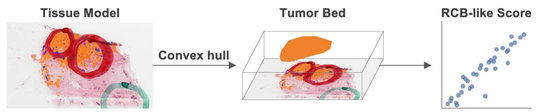

Figure 3. Schematic illustrating use of model-generated tissue region segmentations to derive tumor bed area. The resulting score is "RCB-like" accounting for the lack of corresponding samples from lymph nodes.

- Model predictions were compared with pathologist annotations using Pearson correlation, precision, recall, and F1 metrics.

RESULTS

MODEL PERFORMANCE EVALUATION

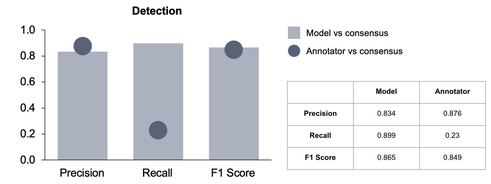

	Model	Annotator
Precision	0.834	0.876
Recall	0.899	0.23
F1 Score	0.865	0.849

Figure 4. Model vs. annotator overall cell detection performance. Cell detection performance evaluated against a ground truth based on exhaustive annotations of 5 pathologists on 120 tissue frames (300 x 300 pixels) from test samples not used in model development (N=536; resections and biopsies). Model and annotator overall cell detection performance in these frames are reported using precision, recall, and F1 metrics.

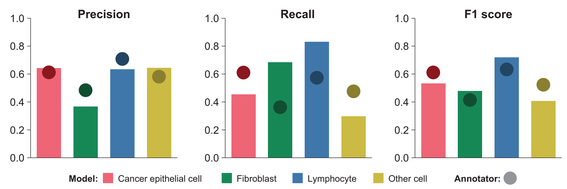

Cell Class	Cell Count
Cancer Epithelial Cell	646
Lymphocyte	1360
Fibroblast	462
Plasma Cell	76
Macrophage	38
Other Cell	854

Figure 5. Model vs. annotator performance in prediction of specific cell classes. Predictions of cancer epithelial cells, fibroblasts, lymphocytes, and other cells evaluated against a consensus ground truth based on exhaustive pathologist annotations on held-out tissue frames. Model vs annotator cell predictions are reported using precision, recall, and F1 metrics.

Table 1. Cell counts for each cell class used to evaluate model performance. The weaker performance shown by the model in detecting macrophages and plasma cells is likely owing to the lower cell counts in these classes.

RESULTS

MODEL PREDICTIONS OF RESIDUAL CANCER BURDEN

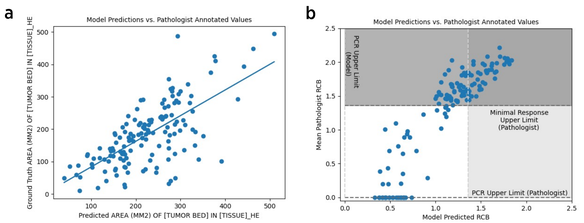

Figure 6. Model vs. annotator predictions of tumor bed area and residual cancer burden. **(a)** Model predictions of tumor bed area were evaluated in comparison to mean measurements from 3 pathologists for each of 145 WSI; Spearman correlation coefficient = 0.63. **(b)** Model predictions of RCB score (based on tumor bed area and cancer cellularity) were evaluated in comparison to mean measurements from 3 pathologists for each of 145 WSI; Spearman correlation coefficient = 0.89.

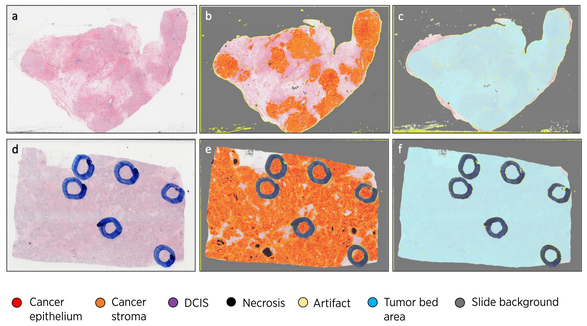

Figure 7. Example H&E images and corresponding model-generated tissue and tumor bed overlays in regions of low and high residual cancer burden. RCB score was determined as the mean of 3 pathologist scores. (a-c) H&E-stained WSI with RCB score I (a) with corresponding tissue overlay (b) and tumor bed overlay (c). (d-f) H&E-stained WSI with RCB score II (d) with corresponding tissue overlay (e) and tumor bed overlay (f).

CONCLUSIONS

CNN model classification of cell types and tissue regions across entire H&E breast cancer WSIs shows concordance with pathologist consensus. Model predictions of tumor bed area, and subsequently derived RCB score, also show concordance with pathologist assessment. These models can be reproducibly applied to quantify diverse histological features in large datasets, potentially enabling improved standardization and efficiency of pathologist evaluation of the breast cancer TME and neoadjuvant response.

AUTHORS

Christian Kirkup[1], Sanjana Vasudevan[1], Filip Kos[1], Ben Trotter[1], Murray Resnick[1], Andrew H. Beck[1], Michael Montalto[1], Ilan Wapinski[1], Benjamin Glass[1], Mary Lin[1], Stephanie Hennek[1] , Archit Khosla[1], Michael G. Drage[1] & Laura Chambre[1]

[1]PathAI, Boston, Massachusetts

contact:
christian.kirkup@pathai.com

REFERENCES

1. Spring, LM et al. Clin Cancer Res. 2020; 26:2838-2848.
2. Hamy, A-S et al. PLoS One. 2020; 15(6): e0234191.
3. Yau, C et al. Lancet Oncol. 2022; 23:149-160.

ACKNOWLEDGMENTS

We thank Bioscience Communications for assistance with figure design. This poster template was developed by SciStories LLC. https://scistories.com/

San Antonio Breast Cancer Symposium, 6-10 December 2022, San Antonio, TX